AD-A084 806   AIR FORCE GEOPHYSICS LAB HANSCOM AFB MA   F/G 22/3
            THE DYNAMICS OF A RIGID BODY IN THE SPACE PLASMA.(U)
            AUG 79   P J WILDMAN
UNCLASSIFIED   AFGL-TR-79-0201   NL

| OF |
AD
A084806

END
DATE
FILMED
6-80
DTIC

AFGL-TR-79-0201
ENVIRONMENTAL RESEARCH PAPERS, NO. 673

LEVEL
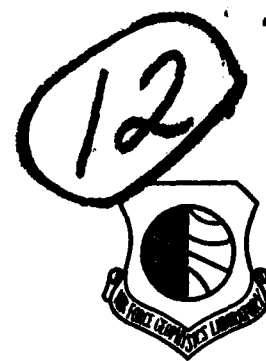
The Dynamics of a Rigid Body in the Space Plasma

PETER J. L. WILDMAN
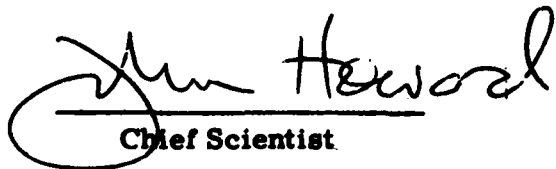
DTIC
SELECTED
MAY 3 0 1980

C

28 August 1979

80 5 28 002

This report has been reviewed by the ESD Information Office (OI) and is releasable to the National Technical Information Service (NTIS).

This technical report has been reviewed and is approved for publication.

FOR THE COMMANDER

Qualified requestors may obtain additional copies from the Defense Documentation Center. All others should apply to the National Technical Information Service.

REPORT DOCUMENTATION PAGE	READ INSTRUCTIONS BEFORE COMPLETING FORM
1. REPORT NUMBER AFGL-TR-79-0201	2. GOVT ACCESSION NO. AD-A084806	3. RECIPIENT'S CATALOG NUMBER

4. TITLE (and Subtitle) THE DYNAMICS OF A RIGID BODY IN THE SPACE PLASMA	5. TYPE OF REPORT & PERIOD COVERED Scientific. Interim
	6. PERFORMING ORG. REPORT NUMBER ERP No. 673

7. AUTHOR(s) Peter J. L. Wildman	8. CONTRACT OR GRANT NUMBER(s)

9. PERFORMING ORGANIZATION NAME AND ADDRESS Air Force Geophysics Laboratory (PH) Hanscom AFB Massachusetts 01731	10. PROGRAM ELEMENT, PROJECT, TASK AREA & WORK UNIT NUMBERS 61102F 2311G203

11. CONTROLLING OFFICE NAME AND ADDRESS Air Force Geophysics Laboratory(PH) Hanscom AFB Massachusetts 01731	12. REPORT DATE 28 August 1979
	13. NUMBER OF PAGES 36

14. MONITORING AGENCY NAME & ADDRESS(if different from Controlling Office)	15. SECURITY CLASS. (of this report) Unclassified
	15a. DECLASSIFICATION DOWNGRADING SCHEDULE

16. DISTRIBUTION STATEMENT (of this Report)

Approved for public release; distribution unlimited

17. DISTRIBUTION STATEMENT (of the abstract entered in Block 20, if different from Report)

18. SUPPLEMENTARY NOTES

Invited contribution to "Space Systems and Their Interactions With the Earth's Space Environment." To be published by AIAA, January 1980, in series "Progress in Astronautics and Aeronautics."

19. KEY WORDS (Continue on reverse side if necessary and identify by block number)

Spacecraft environment interaction
Large space structures
Spacecraft attitude
Spacecraft aerodynamics

20. ABSTRACT (Continue on reverse side if necessary and identify by block number)

The forces resulting from the passage of a conducting body through a partially ionized plasma are reviewed, with emphasis on large space structures. The forces include drag and torque from a number of independent mechanisms, including collisions with neutral and charged particles, solar radiation pressure, and interaction with the earth's magnetic field.

The desirable economic lifetime of tens of years for a large space structure implies an orbital altitude of at least 1000 km, and more probably a ___

R mtc

geosynchronous orbit (6.6 R_e). Drag forces are, therefore, unimportant, except during assembly in low earth orbit and when they generate torque because of a special structure or attitude geometry. For large, long structures with dimensions on the order of kilometers and mass on the order of 10^6 kg or more, the gravity-gradient-induced torque dominates all others, even at geosynchronous-orbit altitudes.

The magnitudes of the various forces are calculated for a non-rotating structure, 2 km long and 10 m wide, at altitudes between 250 km and 36,000 km (6.6 R_e) above the earth.

A short appendix lists additional mechanisms that act when an orbiting body has rotational as well as translational motion.

Preface

I am indebted to Mr. F. Marcos, Dr. M. Smiddy, and Captain H. B. Garrett for several helpful discussions during the preparation of this paper, and to Ms. S. Bredesen for editorial help.

3

Contents

Illustrations

Tables

6

The Dynamics of a Rigid Body in the Space Plasma

1. INTRODUCTION

During the decade of the 1980s, many new types of systems will be placed in orbit around the earth. They will have a number of purposes, the two most probable at the beginning being: facilities, possibly inhabited, for materials production and processing under zero-gravity conditions, and some form of solar-power collector with a means of transmitting that power to earth. From the point of view of the design and on-orbit operation of these "Space Stations," the most dramatic change from the orbiting objects of the 1970s will be their size. Early examples of these systems will have linear dimensions on the order of hundreds of meters up to several kilometers, with sizes projected to reach 10 km by the mid-1990s.[1] With the exception of thin antennas and booms on scientific satellites, no object so far orbited has exceeded a few tens of meters maximum dimension. The structures will be built, initially, by deployment of assemblies from the Space Shuttle cargo bay and, later, by making use of the multiple-flight capability of the Space Shuttle to transport construction materials, fabrication equipment, and workers to a low earth orbit.

In this paper, the interaction between large space structures and their environment will be considered insofar as it produces mechanical perturbing forces

1. Hagler, T., Patterson, H. G., and Nathan, C. A. (1977) Learning to build large structures in space, Astronaut. Aeronaut., 15:51.

that might impact orbital lifetime or, possibly more important in practical terms, the attitude stability and control of such a structure. We will not consider possible techniques of attitude control, but simply demonstrate the kinds of forces that will be present. The structure will be assumed to be rigid, non-rotating (see Appendix A), and any oscillation or deformation caused by the external forces will not be considered at this time. It should be remembered, however, that the accuracy and reliability of attitude control is crucial in some applications, such as solar power transmission to earth. In those cases the structures will have to exhibit rigidity and/or controllability over a wide frequency range of applied forces, and that requirement may well be the deciding factor in the choice of construction and assembly methods.[2]

There are many independently acting physical processes that act upon a body, natural or artificial, passing through the space plasma. Frequently, however, many of these processes result in mechanical or electromechanical forces on the body which are many orders of magnitude smaller than one or two dominant mechanisms, and they may, therefore, be neglected. Exactly which mechanism will exert the greatest force on a body in a specific situation depends primarily on the body's location, size, and geometry. Factors such as solar illumination and spacecraft attitude may cause regular or intermittent changes in the balance of forces acting and these changes can have a cumulative effect, due to resonance with the structure of the body or the dynamics of its orbit.

2. CLASSES OF INTERACTION BETWEEN A MOVING BODY AND A PARTIALLY IONIZED PLASMA

In this section, the "body" (spacecraft or structure) is taken to be electrically conducting, non-magnetic, and to have no rotation about its center of mass (see Appendix A). Unless otherwise stated, no specific geometry is implied. Collisions between particles, charged or neutral, are neglected, because of the very low collision frequencies above about 150 km altitude.

2.1 Charging Effects

2.1.1 SPACECRAFT POTENTIAL (VEHICLE POTENTIAL OR PLASMA POTENTIAL)

Except for transients caused by fluxes of energetic charged particles or by changing solar illumination, there can be no net flux of charge to an isolated body in a partially ionized plasma. Different parts of a spacecraft that are electrically

---

2. Oglevie, R. E. (1978) Attitude control of large solar power satellites, AIAA Paper 78-1266, p. 37, in Proceedings of AIAA Guidance and Control Conference, Palo Alto, CA, 1978, AIAA, New York.

isolated can charge to potentials differing by thousands of volts. This is the case when the spacecraft is in the shadow of the earth at geosynchronous altitudes, due to the low ambient thermal plasma density. Electrical discharge between surfaces can occur when the breakdown voltage is exceeded. If this happens between thin layers of dielectric coatings separating electrical components, for example, it can damage or destroy critical parts of electrical systems. It is the need to eliminate this damage that has been the driving force behind investigations into spacecraft charging mechanisms over the past decade.

The effect of small potentials of 1 V or less also is of interest, because of the drag and torque forces they cause. These forces are caused by the collision and near collision of the charged spacecraft with the ambient plasma particles, and also by the interaction between the ambient magnetic field and currents flowing to and within the spacecraft.

The equilibrium potential Φ of a body in the space plasma is the potential with respect to the plasma at which there is no net flow of charge to or from the body. At this potential Φ, we have:

$$I_- = I_+ + I_s + I_{ph} \, , \tag{1}$$

where I_- is incident electron current

$\quad$ I_+ is incident ion current

$\quad$ I_s is a positive current due to secondary electrons from ion
$\qquad$ and electron impact and from backscattering of incoming
$\qquad$ electrons

$\quad$ I_{ph} is photoemission current.

In order to determine Φ, expressions must be developed for the individual currents constituting Eq. (1). This requires data on the thermal energy plasma, the energetic particle fluxes, and on the backscattering and secondary emission coefficients.[3] In many cases these data are not available, and the usual practice is to use laboratory data or to extrapolate existing space measurements. The full version of Eq. (1) is then solved numerically for Φ. This modeling approach has been used most extensively to establish the equilibrium potential of cylindrical- or spherical-shaped satellites with dimensions of a few meters. In such models, the relatively small disturbing effect of the earth's magnetic field is often neglected; however, the fact that the electrons generally can travel only parallel to the magnetic field places severe limitations on possible electron fluxes in certain

---

3. Knott, K. (1972) The equilibrium potential of a magnetospheric satellite in an eclipse situation, Planet. Space Sci., **20**:1137.

geometries, and must be considered in any detailed treatment of the equilibrium potential.[4,5] Magnetic field effects will be considered further in Sections 2.5 and 2.6.2.

Under most conditions, the polarity and magnitude of Φ depend upon the balance in Eq. (1) between I_{ph}, the total photocurrent, and the portion of I_- that is due to thermal-energy electrons reaching the body. There are, however, two important exceptions to this statement: one concerns spacecraft in geosynchronous orbit under eclipse conditions (spacecraft in the earth's shadow), and the other concerns regions where the thermal plasma density exceeds a value of approximately 5×10^3 cm^{-3}. In the first case, at geosynchronous altitude, particles with energies on the order of several tens of keV frequently are present and impinge on the spacecraft. If electrons predominate in this flux, then in shadow, where no photocurrent is generated to balance this negative flux, the spacecraft will rest at a negative potential of many kilovolts in order both to reduce the electron flux and to attract positive ions as a means of restoring zero net charge flow to the spacecraft. In the second case, at low altitudes in a relatively dense thermal plasma ($N \geq 5 \times 10^3$ cm^{-3}), the isotropic flux of rapidly moving electrons is several orders of magnitude greater than the photocurrent ($i_{ph} \approx 3 \times 10^{-9}$ amp cm^{-2}). It is balanced by the flux of relatively slow moving positive ions swept up by the rapid motion of the spacecraft ($v_s \approx 7 \times 10^5$ cm sec^{-1}), and under these conditions the absence of solar illumination to generate a photocurrent makes little or no difference to the value of the equilibrium potential Φ. This is generally the case at altitudes below about 1500 km where Φ has a value of 1 or 2 V negative, although plasma densities low enough to allow the photocurrent to predominate in Eq. (1) may be encountered below 1500 km in auroral and polar regions. At plasma densities down to a few cm^{-3}, a positive potential of some tens of volts is sufficient to equalize the photocurrent in the absence of high energy particles.

As indicated, extensive studies have been made of the equilibrium conditions of small spherical satellites.[6-8] An important factor in those studies is the extent

4. Chu, C. K., and Gross, R. A. (1966) Alfvén waves and induction drag on long cylindrical satellites, AIAA Journal, 4 (No. 12):2209.

5. Beard, D. B., and Johnson, F. S. (1960) Charge and magnetic field interaction with satellites, J. Geophys. Res., 65:1.

6. Samir, U., and Willmore, A. P. (1966) The equilibrium potential of spacecraft in the ionosphere, Planet. Space Sci., 14:1131.

7. Chang, H. H. C., and Smith, M. C. (1960) On the drag of a spherical satellite moving in a partially ionized atmosphere, Brit. Interplanet. Soc. J., 17:199.

8. Brundin, C. L. (1963) Effects of charged particles on the motion of an earth satellite, AIAA Journal, 1 (No. 11):2529.

to which the plasma is modified by the electrostatic charge and motion of the spacecraft. This falls under the general category of "sheaths and wakes" phenomena, and is of great importance when scientific measurements of the ambient pla.. na are required, since in order to measure charged particles with energies of a few tenths eV the collecting probes must be at the plasma potential.[9] The electrostatic charge on the spacecraft is screened from the ambient plasma by a sheath region where particles of one sign predominate (positive ions in the case of a negatively charged spacecraft). This sheath is characterized by the Debye length (λ_D), which is the distance from the surface at which the potential falls to $1/e$.

$$\lambda_D = \left(\frac{kT_e}{4\pi n_e e^2}\right)^{\frac{1}{2}} \quad cm \tag{2a}$$

$$\lambda_D = 6.9 \left(\frac{T_e}{n_e}\right)^{\frac{1}{2}} \quad cm, \tag{2b}$$

where T_e is thermal electron temperature in $^\circ K$

n_e is electron density in $n\ cm^{-3}$

e is electron charge in Coulomb

k is Boltzmann constant = $1.38 \times 10^{-16}\ erg\ ^\circ K^{-1}$.

The degree of electrostatic screening and the effect of ion and electron thermal velocities in "filling in" any wake region left by the rapid passage of the spacecraft through the plasma must be considered in an exact evaluation of equilibrium conditions.[8,10] Since they are essentially edge effects, however, sheaths and wakes have little impact on the mechanical forces acting on an extensive planar structure in the space plasma, except when very high voltages —

9. Samir, U., Maier, E. J., and Troy, B. E. Jr. (1973) The angular distribution of ion flux around an ionospheric satellite, J. Atmos. Terr. Phys., 35:513.

10. Kasha, M. A. (1969) The Ionosphere and its Interaction With Satellites, Chap. 3, New York, Gordon and Breach.

11

on the order of thousands of volts—are generated (as on a solar power station).[11, 12]

We note here, for completeness, the equation for Φ for a conducting sphere, radius R in the 150 km to 1500 km altitude range. At such altitudes Φ is generally negative, and the local Debye length is small compared with the dimensions of the sphere. Neglecting wake effects and the presence of the earth's magnetic field, Φ is given by Brundin[8] as:

$$\Phi = \frac{kT_e}{2e}\left\{ \ln\left(\frac{8kT_e}{\pi m_e v_s^2}\right) - 2\ln\left(1 - \frac{I_{ph}}{v_s \pi R^2 n_e e}\right)\right\},\tag{3}$$

where v_s is the satellite volocity

m_e is electron mass

I_{ph} is the total photoelectron current.

2.1.2 PLANAR SURFACE CURRENT FLOW

When considering large-scale conducting structures, it is necessary to consider the different potentials that are induced at different locations on the structure by its motion through the earth's magnetic field (Section 2.5). Currents of different polarities and area densities, therefore, flow through the surface at different locations on the structure. As these currents flow within the structure, they cause drag, and possibly torque, as they interact with the ambient magnetic field. We quote here expressions for the currents flowing from a Maxwellian plasma to a planar surface at known potential for both accelerating and retarding modes, neglecting edge effects.[13] These currents must be evaluated so that the flow pattern within the structure can be used to calculate the resulting magnetically induced drags and torques.

11. Parker, L. W. (1979) Plasma sheath effects and voltage distributions of large, high-power satellite solar arrays, _Proceedings of the Spacecraft Charging Technology Conference, USAF Academy, Colorado Springs, Colo., 1978_, p. 341, NASA Conference Publication 2071/AFGL-TR-79-0082.

12. Freeman, J. W., Cooke, D., and Reiff, P. (1979) Space environmental effects and the solar power satellite, _Proceedings of the Spacecraft Charging Technology Conference, USAF Academy, Colorado Springs, Colo., 1978_, p. 408, NASA Conference Publication 2071/AFGL-TR-79-0082.

13. Whipple, E. C. Jr. (1959) The ion-trap results in the 'exploration of the upper atmosphere with the help of the third Soviet Sputnik,' _Proc. IRE_, 47:2023.

In an accelerating mode (Φ positive for electrons and negative for ions), the current flowing to area A is given by:

$$I_{acc} = \frac{neA}{\sqrt{\pi a}} \left\{ \frac{\sqrt{\pi}}{2} \gamma \, \cos\theta \, [1 + \mathrm{erf}(\gamma \cos\theta)] + \frac{1}{2} \exp[-\gamma^2 \cos^2\theta] \right\}. \tag{4}$$

In a retarding mode (Φ negative for electrons and positive for ions),

$$I_{ret} = \frac{neA}{\sqrt{\pi a}} \left\{ \frac{\sqrt{\pi}}{2} \gamma \, \cos\theta \, [1 - \mathrm{erf}(x - \gamma \cos\theta)] + \frac{1}{2} \exp[-(x - \gamma \cos\theta)^2] \right\} \tag{5}$$

$$x = \sqrt{e\Phi/kT} \tag{6}$$

$$a = m/2kT \tag{7}$$

$$\gamma = v_s/\sqrt{a}, \tag{8}$$

where e   is electron charge

n   is density of the particles

m   is mass of a particle

T   is Maxwellian temperature of the particles

k   is Boltzmann constant

Φ is potential difference of surface relative to plasma

A   is area of the surface

v_s is velocity of the surface relative to plasma

θ is angle between the surface normal and v_s .

2.2 Solar Radiation Pressure

Any object in sunlight will be subjected to a force caused by momentum transfer from solar photons to any surface that they strike. For an earth satellite in a circular orbit that does not enter the earth's shadow, the net acceleration due to solar radiation pressure is zero, since the force is accelerating for one-half the orbit and retarding for the other half. For a body in an elliptic orbit that enters the earth's shadow, there will be a net change in the energy of the body due to solar radiation pressure, unless the accelerating and retarding radiation pressure forces are equal over a complete orbit. This is a geometry that cannot persist for an extended period, because of the shift of the orbit in inertial space; therefore, radiation pressure must be considered in the calculation of most orbital dynamics. For interplanetary missions, the radiation pressure may be in the same sense for extended periods and can be harnessed to accelerate, slow

13

down, or stabilize probes during long, otherwise unpowered, coasting phases.[14] It can even be used as the primary means of propulsion, as in the NASA solar sail proposal to carry a payload to rendezvous with Halley's comet.

If the area presented to solar radiation is asymmetric about the body's center of mass, a torque will be applied even in orbits where radiation pressure causes no net acceleration of the center of mass. This mechanism can be the principal cause of applied torque, especially in the case of a structure that projects large optically opaque surfaces to solar radiation (as opposed to one with an open structure). It would be possible, under some orbital and spacecraft configurations, to balance out magnetic and/or aerodynamic torques by careful positioning and trimming of open and closed areas. The feasibility of using solar radiation pressure to trim spacecraft attitude has already been demonstrated on the OTS-2 geosynchronous satellite.[15] (A small additional force under conditions of solar illumination arises from the recoil of the solar-induced photoelectrons from the body. This is on the order of 1 percent of the true radiation pressure and may be neglected.)

For a perfectly absorbing surface, the radiation pressure is equal to the energy density of solar radiation, and the force acting on a body is given by:

$$F_R = \frac{L}{4 \pi R_s^2 c} A \cos \alpha \quad \text{dyne,} \tag{9a}$$

where L is total energy radiated from the sun (3.86×10^{33} erg cm^{-2} sec^{-1})

$\quad R_s$ is distance from the sun in cm

$\quad c$ is velocity of light (3×10^{10} cm sec^{-1})

$\quad A$ is area exposed to solar radiation

$\quad \alpha$ is angle between the normal to A and the sun-body line.

In the neighborhood of the earth, $R_s = 1$ AU (1.495×10^{13} cm) and the radiation pressure C_r is given by:

$$C_r = 4.6 \times 10^{-5} \cos \alpha \quad \text{dyne cm}^{-2}. \tag{9b}$$

14. Sohn, M. (1959) Attitude stabilization by means of solar radiation pressure, Am. Rocket Soc. J. 29:371.

15. Renner, U. (1979) Attitude control by solar sailing - a promising experiment with OTS-2, European Space Agency Journal 3:35.

2.3 Neutral Particle Drag

Below about 400 km altitude, the largest contribution to spacecraft decelera-
tion comes from collisions with the neutral constituents of the atmosphere, which
greatly outnumber the charged particles in these regions. Conditions at all prac-
tical altitudes for spacecraft, above about 150 km, are those of "free molecular
flow," meaning that the mean free path of all particles is much greater than the
dimensions of the body with which they interact. Additionally, for regions where
neutral particle collisions are significant, their thermal velocities are much
lower than the velocity of the spacecraft $(v_s \approx 7 \times 10^5$ cm sec$^{-1})$. The magnitude
of the drag force under these conditions is given by:

$$F_{ND} = \frac{1}{2} \rho \, v_s^2 C_D A \quad \text{dyne,} \tag{10}$$

where F_{ND} is the drag force

ρ is the neutral atmosphere density in gm cm^{-3}

v_s is the spacecraft velocity in cm sec^{-1}

C_D is the drag coefficient

A is cross-sectional area projected into the flow in cm^2.

The value of C_D depends upon the geometry of the body, the mode of reflection of
the incoming particles (specular or diffuse), and the degree of thermal accomoda-
tion of the particles to the surface temperature of the body. A value of 2.2 is
generally used for C_D for spherical and nearly spherical bodies in the 150 to
400 km altitude range. Shapes such as flat plates and cylinders have somewhat
higher values of C_D, although this is also dependent on the reflection processes.[16]
At higher altitudes, above about 600 km, the thermal velocity of all particles,
neutral and charged, must be considered;[17] C_D rises to a value of greater than
4.0, and the drag process becomes more efficient.[16, 18] Because of the much
greater degree of ionization at these higher altitudes, however, the relative con-
tribution of neutral particle collisions to the total drag becomes very small.

16. Cook, G. E. (1965) Satellite drag coefficients, Planet. Space Sci. 13:929.

17. *Schamberg, R. (1959) Analytic representation of surface interaction for free
molecule flow with application to drag of various bodies, in Aerodynamics
of the Upper Atmosphere, edited by D. J. Masson, p. 12-1, Rand
Corporation.*

18. Epstein, P. S. (1924) Resistance experienced by spheres in their motion
through gases, Phys. Rev. 23:710.

2.4 Charged Particle Drag (Coulomb Drag)

2.4.1 DIRECT IMPACT DRAG

The potential of the spacecraft modifies the trajectories of charged particles that otherwise would not strike it. Since electrons may be neglected in drag calculations, due to their low mass compared with any ion, the usual situation is that the effective collisional area of the spacecraft is increased by the attraction of positive ions to a negatively charged body, and decreased by a positively charged body.

In the simplest case, for a spherical body moving at $v_s \geq \geq v_i$ where v_i is the ion thermal velocity, and when all ions stick to the body after impact and neutralization, the drag is simply:

$$F_{ID} = \frac{1}{2} \pi m_i n_i v_s^2 r_e^2 \quad \text{dyne,} \qquad (11)$$

where m_i is ion mass in gm

n_i is ion density in n cm^{-3}

v_s is the satellite velocity in cm sec^{-1}

r_e is effective radius for ion collection in cm.

From consideration of momentum conservation, r_e is given by:

$$r_e = R \left[1 + \frac{2e\,\Phi}{m_i v_s^2} \right]^{\frac{1}{2}} \quad \text{cm,} \qquad (12)$$

where R is the radius of the spherical body and Φ is the spacecraft potential.

The exact determination of the effect of spacecraft charge depends upon the degree to which the charge is screened from the surrounding plasma. This is usually defined in terms of the local Debye length (λ_D), but it must be remembered that this is the distance at which the potential due to spacecraft charge is reduced by $1/e$, and it is not the limit of the disturbed region. Where λ_D is more than a few centimeters, the disturbed region around the spacecraft can be on the order of 10 to 40 percent of the total cross section of a spacecraft 1 or 2 m in diameter.[8]

At impact, the ions are neutralized and, if re-emitted, carry momentum that is a further source of drag if the reflection mechanism is diffuse.[17] This re-emission drag can be greater than the initial impact drag of the ions if there is no

16

thermal accommodation of the incident particles to the body surface temperature. This drag has a maximum value, F_r, given by Brundin[8] as:

$$F_r = n_i m_i v_s^2 \pi R^2 \left(1 + \frac{2e\,\Phi}{m_i v_s^2} \right) \left\{ \frac{4}{9} \left[1 + \left(\frac{2e\,\Phi}{m_i v_s^2} \right)^{1/2} \right] \right\} \text{dyne}. \tag{13}$$

where n_i is ion number density in n cm^{-3}

m_i is ion mass in gm

R is the spherical body radius in cm

Φ is spacecraft potential in volts

v_s is the satellite velocity in cm sec^{-1}.

2.4.2 NON-COLLISIONAL DRAG (MAXWELL DRAG OR DYNAMIC FRICTION)

An additional source of charged particle drag arises from Coulomb interaction leading to momentum exchange between a charged body and ions that do not strike it but whose trajectories are changed. A critical factor in determining this drag is, again, the extent to which the effect of spacecraft potential penetrates into the ambient plasma. The problem has been approached by a number of workers[7, 19, 20] who made varying assumptions about the extent and geometry of the electrostatic screening of a body moving through a plasma; however, in considering large structures, we need note only that non-collisional drag is a significant fraction of the total charged-particle drag only when the body in question has dimensions no more than an order of magnitude greater than the local Debye length.[21] In regions where this condition is satisfied, for very large structures in geosynchronous orbit outside the plasmapause, for example, ion densities are too low (< 10 cm^{-3}) to contribute any significant drag.

2.5 Magnetic Field Drag Effects

The effects of the earth's magnetic field on the potential distribution and current flows on a conducting body in the space plasma are not significant in practice

19. Jastrow, R., and Pearse, C. A. (1957) Atmospheric drag on the satellite, J. Geophys. Res. 62:413.

20. Fournier, G. (1970) Electric drag, Planet. Space Sci. 18:1035.

21. Knechtel, E. D., and Pitts, W. C. (1964) Experimental investigation of electric drag on satellites, AIAA Journal, 2 (No. 6):1148.

unless the dimensions of the body exceed approximately 10 m. As linear dimensions increase, the potentials generated on the body by its motion across the magnetic field begin to exceed the energies of the plasma particles with respect to the body. These usually lie within the range of $\pm$ 25 eV. Ions and electrons flow preferentially to the negative and positive sections of the body; therefore, although there is a zero net current flow to the whole body, positive and negative currents flow to and within specific parts of the body. This results in drag (Lorentz forces) on the body as the various currents interact with the ambient magnetic field.

For a conducting body, as shown in Figure 1, with length $2L_x$ perpendicular to v_s and B, a potential E_x will be set up along the length of the body:

$$E_x = 10^{-8}(v_s \times B) \quad \text{volts cm}^{-1}, \tag{14}$$

where

$\quad$ v_s is in cm sec^{-1}

$\quad$ B is in gauss.

Figure 2 shows the distribution of the currents that will flow, partly as a result of this potential and partly due to collisions with ambient ions and electrons, when L_x is on the order of a few meters. The induction drag or Lorentz force (F_L) acting on the body as a result is:

$$F_L = B \int_{-L_x}^{+L_x} I(x)\sin \delta \, dx \quad \text{dyne}, \tag{15}$$

where $I(x)$ is the net current flowing in an increment dx of the body located at x

$\quad$ δ is the angle between the direction of current flow and the magnetic field B.

For the configuration of Figure 1, $\delta = 90^\circ$, and if the currents are equally distributed about the center of the structure, they flow for an average distance of L_x perpendicular to B, hence:

$$F_L = 10^{-1} I B L_x \quad \text{dyne}, \tag{16}$$

where I is the mean current in amps
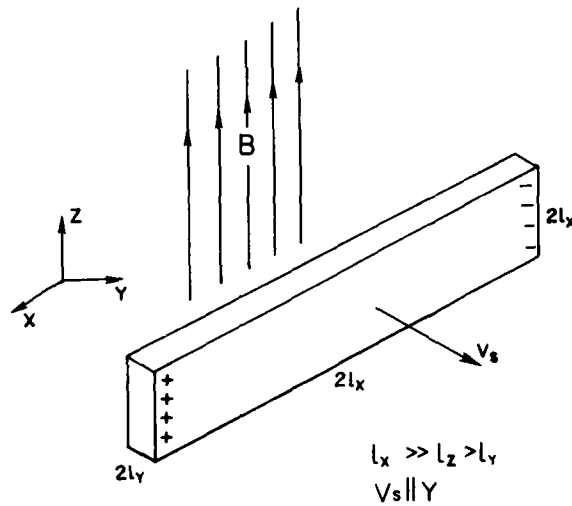
$\quad$ B is in gauss

$\quad$ L_x is in cm.

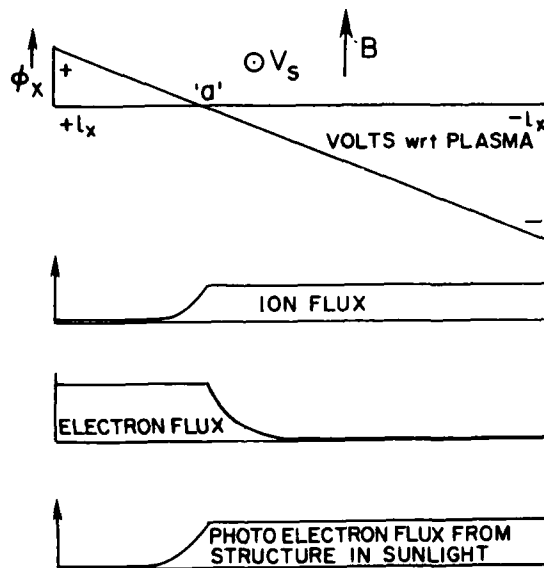Figure 1. The Basic Structure Moving Perpendicular to the Local Magnetic Field

Figure 2. The Current and Potential Distributions Along the x Axis of the Structure, When l_x is on the Order of a Few Meters

19

The location of "a," the point on the structure that rests at plasma potential, is determined by balancing the electron flux to the positive part of the structure with the ion flux to the negative part and the photocurrent (positive) emitted predominantly from the negative section. Since the electron flow to the structure is parallel to the magnetic field, current densities and distributions depend on the orientation of the structure.

At altitudes where plasma densities are approximately 5×10^3 cm^{-3} or greater, point "a," for structures no more than a few meters in size, is generally located between one-third and one-half of the length of the structure from the positive end. As the linear size is increased along the x axis, higher potentials are induced across the structure and the positive end is effectively grounded in the local plasma; that is to say, $a > L_x$.[4] At higher altitudes for structures of all sizes, the photocurrent is significantly greater than either the ion or electron flux. The entire strucutre rests at a positive potential with respect to the plasma and attracts an increased flux of electrons to balance the photocurrent. Electrons still flow preferentially to the less negative end of the structure, and the magnetically induced potential across the structure will still be generated.

2.6 Torque Processes

All the drag processes outlined so far also will exert a torque on the body if the forces produced have a non-zero total moment about the body's center of mass. Torque also will be generated in the presence of a magnetic field by current loops within the body, but, in this case, no additional drag results as long as the magnetic field is uniform over the dimensions of the body. This process may have serious consequences when dealing with large structures such as solar power stations, where very large currents are generated. Careful routing of current paths is required to minimize the total magnetic moment of the structure.

2.6.1 MOMENTUM TRANSFER TORQUES (PARTICLE IMPACTS AND RADIATION PRESSURE TORQUES)

If a drag process results in a force P per unit area projected in the direction of the body's velocity vector v_s, then the total torque T_p is:

$$T_p = P \iint r \, dA \, \cos \theta \, dr \quad \text{dyne cm,} \tag{17}$$

20

where P is drag pressure in dynes cm^{-2}

r is vector distance of dA, from center of mass in cm

dA is element of surface area in cm^2

v_s is velocity in cm sec^{-1}

θ is the angle between v_s and the normal to dA.

2.6.2 MAGNETIC TORQUES (INDUCTION TORQUES)

When induction drag results from currents flowing through the body from the space plasma, a torque T_L will result if there is a net non-zero moment of these drag forces about the center of mass. From Eq. (15) we obtain:

$$T_L = 10^{-1} B \int_{-L_x}^{+L_x} I(x) L_x \sin \delta \, dx \quad \text{dyne cm,} \tag{18}$$

where B is magnetic field in gauss

$I(x)$ is current in amps flowing in an element dx located at L_x cm from the center of mass

δ is the angle between the direction of current flow and the magnetic field.

In addition, a current flowing around a closed loop in the presence of a uniform magnetic field generates a torque given by:

$$T_i = 10^{-1} I A B \sin \alpha' \quad \text{dyne cm,} \tag{19}$$

where I is current around loop in amps

A is area enclosed by loop in cm^2

B is magnetic field in gauss

α' is angle between the magnetic field and the normal to the plane of the loop.

2.6.3 GRAVITATIONAL TORQUE

The gravitational potential gradient of the earth exerts a torque on a body in such a way that its axis of minimum moment of inertia aligns itself with the radius through the center of the earth; that is to say, the long axis of a body will line up with the local vertical. Use is made of this torque in the technique of "gravity

21

gradient stabilization" for satellites that are required to present the same side toward the earth at all times. Stabilization is achieved by extending a mass at the end of a long boom erected along the axis required to point downwards. This greatly increases the moments of inertia about the axes perpendicular to the boom, which then aligns itself along the local vertical. [22]

Gravitational torques have had little effect on the stability and alignment of many satellites launched to date because of their relatively small overall dimensions, and the fact that their moments of inertia about all three axes are frequently of the same order of magnitude. In addition, antennas and solar-cell arrays have made large relative contributions to the cross-sectional area of the spacecraft compared with small additions to moments of inertia. Because of this, particle impacts, magnetic induction effects, and, at higher altitudes, solar radiation pressure, have been the principal sources of torque. This situation is changed, however, when we consider massive, elongated structures with high transparencies for particle collision and solar radiation pressure.

Figure 3 shows the previous sample structure aligned at an angle θ to the local vertical r such that x, z, and r are coplanar. The gravitational torque T_y about the y axis is given by Thomson[23] as:

$$T_y = \frac{3GM}{2R^3} \left[(MI)_z - (MI)_x \right] \operatorname{Sin} 2\theta \quad \text{dyne cm,} \tag{20}$$

where G is universal gravitation constant $= 6.67 \times 10^{-8}$ dyne cm^2 gm^{-2}

M is mass of the earth $= 5.973 \times 10^{27}$ gm

R is distance to center of the earth in cm

$(MI)_{x,z}$ are moments of inertia about x and z axes in gm cm^2

θ is the angle between the local vertical r, and the x axis of the structure.

22. Fischell, R. E., and Mobley, F. F. (1964) A system for passive gravity - gradient stabilization of earth satellites, in Progress in Astronautics and Aeronautics: Guidance and Control - II, Vol. 13, p. 37, New York, Academic Press.

23. Thomson, W. T. (1962) Spin stabilization of attitude against gravity torque, J. Astronaut. Sci. 9:31.
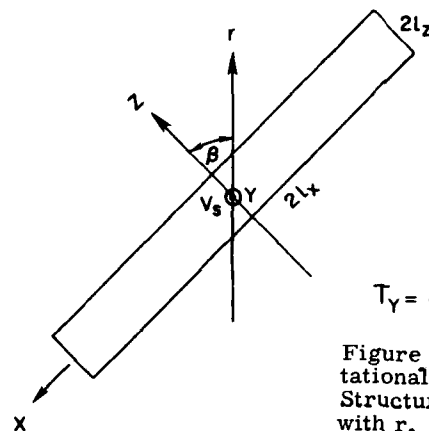
GRAVITATIONAL TORQUE:

$$T_Y = \frac{3GM}{2R^2}\left[(mI)_z - (mI)_x\right] \sin 2\theta$$

Figure 3. Geometry to Produce a Gravitational Torque About the y Axis of the Structure. The x and z axes are coplanar with r, the local vertical

3. NUMERICAL EXAMPLES — DRAG

In this section we calculate values for the drag forces on a sample structure that are generated at a number of altitudes by the processes outlined in Section 2. Representative values of environmental parameters are given in Table 1 for an exospheric temperature of $1500°K$. The structure is as shown in Figure 1 and its dimensions, mass, and velocity at the various altitudes are given in Table 2.

Table 1. Environmental Parameters

	250	500	1,000	$36,000(6.6R_e)$
Altitude (h km)	250	500	1,000	$36,000(6.6R_e)$
Neutral Density (ρ gm cm^{-3})	10^{-13}	3×10^{-15}	2×10^{-13}	---
Neutral Density (N cm^{-3})	10^9	10^8	10^5	---
Plasma Density (n_i cm^{-3})	5×10^5	10^6	3×10^4	$5\times10^0 - 5\times10^2$
Neutral Temperature ($T_i \approx T_n$ °K)	800	1,000	2,000	5,000 - 20,000
Electron Temperature (T_e °K)	1,000	1,500	2,000	5,000 - 20,000+ (inside plasmasphere) Several keV (outside plasmasphere)
Mean Ion Mass ($\overline{m}$ amu)	24	16	8	1
Debye length (λ_D cm)	0.3	1.0	2.0	200+
Geomagnetic Field (B gauss)	0.45	0.40	0.33	10^{-3}

Table 2. Structure Details

Dimensions (cm):	Length	$(2L_x)$	2×10^5
	Height	$(2L_z)$	10^3
	Thickness	$(2L_y)$	$< 10^2$
	Total Projected Area	$(2L_x \times 2L_z \ cm^2)$	2×10^8
	Mass per Unit Projected Area $(gm \ cm^{-2})$		10^1
	Total Mass (gm)		2×10^9
Velocity $(cm \ sec^{-1})$:		250 km	7.80×10^5
		500 km	7.60×10^5
		1,000 km	7.35×10^5
		36,000 km	3.00×10^5

3.1 Solar Radiation Pressure

In the near-earth region (1 AU), the value of solar radiation pressure is effectively constant at all altitudes. For a totally absorbing surface, the pressure is:

$$C_r = 4.6 \times 10^{-5} \ \text{Cos} \ \alpha \quad \text{dyne} \ cm^{-2} \tag{9a}$$

If the structure faces directly toward the sun, $\alpha = 0^\circ$ and the total force acting on an area of $2 \times 10^8 \ cm^2$ will be:

$$4.6 \times 10^{-5} \times 2 \times 10^8 = 9.2 \times 10^3 \ \text{dyne}.$$

24

3.2 Neutral Particle Drag

The neutral particle drag is a decelerating force, acting at all times in the opposite direction to the velocity vector v_s:

$$F_{ND} = \frac{1}{2} \rho v_s^2 C_D A. \tag{10}$$

From Section 2.3, the Drag Coefficient, C_D, = 2.2, and the area projected into the velocity vector, A, = 2×10^8 cm^2. The neutral drag at three altitudes is shown in Table 3. Neutral densities are considered negligible at geosynchronous orbit. Note that at an altitude of 1000 km the neutral component is already less than the solar radiation pressure drag (Section 3.1) at the time when the strucutre is facing directly into the sun; the net energy transfer due to solar radiation pressure, however, is very close to zero over a complete orbit.

Table 3. Neutral Drag

h (km)	250	500	1000
ρ (gm cm^{-3})	10^{-13}	3×10^{15}	2×10^{-17}
v_s (cm sec^{-1})	7.8×10^5	7.6×10^5	7.35×10^5
F_{ND} (dyne)	1.34×10^7	3.81×10^5	2.38×10^3
F_{ND}/A (dyne cm^{-2})	6.69×10^{-2}	1.91×10^{-3}	1.19×10^{-5}

3.3 Charged Particle Drag

The charged particle drag is a decelerating force acting in the same sense as neutral particle drag:

$$F_{ID} = \frac{1}{2} m_i n_i v_s^2 A \quad \text{dyne}, \tag{21}$$

where m_i is mean mass of ambient ions in gm

n_i is number density of ambient ions in n cm^{-3}

v_s is the spacecraft velocity in cm sec^{-1}

A is the area projected into v_s in cm^2.

The values of drag given in Table 4 are derived from Eq. (21) for a structure of cross-sectional area $A = 2 \times 10^8$ cm^2 moving much faster than the thermal velocity of the ions. No allowance is made for increased effective area due to Coulomb attraction of nearby ions, since that is most significant when the dimensions of the structure are no more than one order of magnitude greater than the local Debye length. Similarly, no diffuse re-emission of the neutralized ions is considered. Since both of these factors would increase charged particle drag, the figures given in Table 4 are conservative. Since thermal ion velocities at geosynchronous orbit are greater than orbital velocity, Eq. (21) does not apply; however, the ambient density is so low at this altitude that the drag resulting from ion impact is negligible compared with solar radiation pressure forces.

Table 4. Charged Particle Drag

h (km)	250	500	1000
m_i (gm)	4.01×10^{-23}	2.68×10^{-23}	1.34×10^{-23}
n_i (n cm^{-3})	5×10^5	10^6	3×10^4
v_s (cm sec^{-1})	7.8×10^5	7.6×10^5	7.35×10^5
F_{ID} (dyne)	1.22×10^3	1.54×10^3	2.17×10^1
F_{ID}/A (dyne cm^{-2})	6.1×10^{-6}	7.73×10^{-6}	1.08×10^{-7}

3.4 Magnetic Drag (Induction Drag)

The three processes dealt with so far all depend on the area that the structure projects into the velocity vector or the sun vector. If an open-girder type of construction is used, the forces resulting from these processes would be reduced in direct proportion to the optical transparency of the area projected. This change in optical transparency must be uniform over the whole structure, however, or a torque will result.

In the case of magnetic field drag (induced drag), it is the linear dimensions and orientation of the structure in the local magnetic field that are critical. From Eq. (16), the drag for the orientation in Figure 1 is:

$$F_L = 10^{-1} \, I \, B \, L_x \quad \text{dyne.} \tag{16}$$

In practice, the actual value of I depends upon the local ion density, solar illumination, transparency, the velocity of the structure, and on orientation in the magnetic field as it affects the potential distribution over the structure. For this example we consider only the photocurrent (I_p) due to solar UV photons and the ion collection current (I_i) swept up by the structure whose velocity is assumed to be large compared with the ion thermal velocities. This assumption is not true at geosynchronous orbit altitudes where the photocurrent dominates. In an equatorial orbit, the photocurrent contribution will be zero at 1200 hr LT, and maximum at 0600 hr LT and 1800 hr LT, if both back and front surfaces are taken to be photoemitters. If almost all of the surface of the structure is an ion collector and/or a photoemitter, then the average distance perpendicular to B through which these currents flow will be close to L_x (= 10^5 cm), one-half the total length. At each altitude we find I_i, using the environmental data in Table 1, and then substitute in Eq. (16) to determine F_L. Photocurrent I_p = 6 x 10^{-1} amp at all altitudes, and its variation around the orbit is reflected in the range of values for I_i given in Table 5.

Table 5. Induction Drag

h (km)	250	500	1000	36000
I_i (amp)	$(1.25-1.31) \times 10^{-1}$	$(2.43-2.49) \times 10^1$	$(7.06-13.06) \times 10^{-1}$	6×10^{-1}
B (gauss)	4.5×10^{-1}	4.0×10^{-1}	3.3×10^{-1}	10^{-3}
F_L Max (dyne)	5.9×10^4	9.96×10^4	4.32×10^3	6×10^0
F_L/A (dyne cm^{-2})	2.94×10^{-4}	4.98×10^{-4}	2.16×10^{-5}	3×10^{-8}

4. NUMERICAL EXAMPLES – TORQUE

4.1 Momentum Transfer Torques

In order to estimate the magnitude of these torques (due to solar radiation pressure and collisions with charged and neutral particles), we modify the structure as shown in Figure 4. One-quarter of the length is covered with a conductor, as before, but the remainder now has an open construction with an optical transparency of 90 percent. The total mass and its distribution about the center of gravity remains unchanged. The y axis of the structure is maintained parallel to v_s at all times.

27
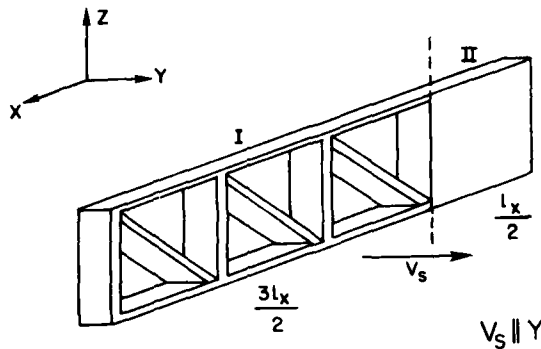
OPTICAL TRANSPARENCY
SECTION I = 90%
SECTION II = 0%

Figure 4. Modification of the Basic Structure to-
Demonstrate Momentum Transfer and Solar Radia-
tion Pressure Torques by the Imbalance of Forces
About the Center of Gravity

The applied torque will have a maximum value when the structure is moving directly towards the sun. The solar radiation pressure component varies continuously *throughout the orbit and acts to equalize the particle impact torques* whenever v_s has a component away from the sun.

If the pressure on the structure at any time is P dyne cm^{-2}, then from Eq. (17) the resulting torque T_p will be:

$$T_p = 2 L_z P \int_{-L_x}^{+L_x} L_x \, dL_x \quad \text{dyne cm.} \tag{22a}$$

Due to the basic symmetry about the z axis, T_p arises from the additional area in the enclosed section of the structure so that:

$$T_p = 0.9 \left\{ 2 L_z P \left[\frac{L_x^2}{2} - \frac{L_x^2}{8} \right] \right\} \tag{22b}$$

$$T_p = 3.38 \times 10^{12} \text{ P dyne cm.}$$

From Section 3 we obtain maximum values for P in Table 6 by adding solar radiation pressure and the neutral and charged particle forces.

28

Table 6. Pressure Torque

h (km)	250	500	1000	36000
P(dyne cm^{-2})	6.69×10^{-2}	1.91×10^{-3}	5.80×10^{-5}	4.6×10^{-5}
T_p(dyne cm)	2.26×10^{11}	6.46×10^{9}	1.96×10^{8}	1.56×10^{8}

4.2 Magnetic Torques (Induction Torques)

As an example of currents flowing in a section of the structure to produce a torque by imbalance about the center of mass, we will use the currents derived in Section 3.4. We reduce them by a factor of 4 to represent their flowing in the enclosed portion of the structure, and ignore currents flowing in the rest of the structure. The mean moment arm of the Lorentz forces produced about the center of mass will be $3L_x/4$, and the currents will flow for a mean distance of $L_x/4$ perpendicular to B. In Table 7 we use these values in Eq. (18) to obtain T_L.

Table 7. Induction Torque

h (km)	250	500	1000	36000
I (amp)	3.28×10^{0}	6.23×10^{0}	3.27×10^{-1}	1.50×10^{-1}
B (gauss)	4.5×10^{-1}	4.0×10^{-1}	3.3×10^{-1}	10^{-3}
T_L (dyne cm)	2.77×10^{8}	4.67×10^{8}	2.03×10^{7}	2.81×10^{4}

To estimate the torque (T_i) caused by a flow of current around a closed loop within the structure, we postulate a net current of 1 amp flowing around the outermost edges of the structure, aligned as in Figure 1, so that the torque acts about the x axis of the structure. Note that for this source of torque internal construction and optical transparency are irrelevant; the torque is determined by the area enclosed by the loop and its alignment in the magnetic field. In Table 8 we use Eq. (19) and Table 1 to obtain values for T_i.

Table 8. Current Loop Torque

h (km)	250	500	1000	36000
B (gauss)	4.5×10^{-1}	4.0×10^{-1}	3.3×10^{-1}	10^{-3}
T_i (dyne cm)	9.0×10^{6}	8.0×10^{6}	6.6×10^{6}	2×10^{4}

4.3 Gravitational Torque (Gravity Gradient)

Starting with the structure in Figure 4 aligned at $\beta = 45°$ to the local vertical, we determine the gravitational or gravity gradient torque for the four altitudes.

Taking mass and dimensions from Table 2 we have, since $I_x >> I_z$ and $I_z > I_y$:

$$(MI)_y \approx (MI)_z$$
$$= 6.67 \times 10^{18} \text{ gm cm}^2$$
$$(MI)_x = 1.67 \times 10^{14} \text{ gm cm}^2.$$

Substituting in Eq. (20) we obtain the values for T_y given in Table 9.

Table 9. Gravitational Torque

h (km)	250	500	1000	36000
T_y (dyne cm)	1.37×10^{13}	1.23×10^{13}	9.94×10^{12}	5.40×10^{10}

5. CONCLUSIONS

The most striking result from the evaluation of forces acting on a large space structure is the greatly increased importance of gravitational torques. At all altitudes considered, this mechanism produces a torque at least 2 orders of magnitude greater than any other. A gravity gradient stabilization mode is, therefore, unavoidable, unless either a continuously operating active attitude control system is used or the structure is designed to have nearly equal moments of inertia about all three axes.[2]

In the first case, the mass of the structure ($10^9 - 10^{11}$ gm) means that large amounts of power would be required for such a system and that the interaction between the control system and the inevitable flexing of so large a structure would pose totally new problems.[24] The equalization of moments of inertia approach seems more promising if gravitational alignment is undesirable; however, if any other mechanism is employed to orient all or part of a structure (solar radiation

24. Ginter, S., and Balas, M. (1978) Attitude stabilization of large flexible spacecraft, AIAA Paper No. 78-1285, in Proceedings of AIAA Guidance and Control Conference, Palo Alto, CA, 1978, AIAA, New York.

pressure using large, light, movable "sails," for example), the situation is complicated by the need for sensing and moving systems that must operate continuously.

Drag forces are of little significance in practice, except perhaps during the assembly phase in low earth orbit. This is because of the need to ensure an orbital lifetime on the order of tens of years, which means that most structures will be placed in final orbits above 1000 km. Since so many structures together with an ever-increasing number of communications satellites and relay platforms will be placed in geosynchronous orbit, plans must be made at this early stage concerning the final disposal of the structures at the end of their useful life ("solar sailing" to much higher orbits, for example). Additionally, contingency plans must be made to minimize the possibility of the re-entry of large substructures that experience some malfunction during assembly, since at space shuttle altitudes orbital lifetimes are no more than a few years.

Great care must be exercised in applying the results of Sections 3 and 4 to other structures and orbits. In most examples the orientation of the structure has been chosen to maximize the individual drag and torque forces. It is possible that other combinations of attitude, geometry, and orbit could combine to reduce the very large differences in the magnitude of the various forces.

References

1. Hagler, T., Patterson, H. G., and Nathan, C. A. (1977) Learning to build large structures in space, Astronautics and Aeronautics, 15:51.

2. Oglevie, R. E. (1978) Attitude control of large solar power satellites, AIAA Paper 78-1266, p. 37, in Proceedings of AIAA Guidance and Control Conference, Palo Alto, CA, 1978, AIAA, New York.

3. Knott, K. (1972) The equilibrium potential of a magnetospheric satellite in an eclipse situation, Planetary and Space Science, 20:1137.

4. Chu, C. K., and Gross, R. A. (1966) Alfvén waves and induction drag on long cylindrical satellites, AIAA Journal, 4 (No. 12):2209.

5. Beard, D. B., and Johnson, F. S. (1960) Charge and magnetic field interaction with satellites, J. Geophys. Res., 65:1.

6. Samir, U., and Willmore, A. P. (1966) The equilibrium potential of spacecraft in the ionosphere, Planetary and Space Science, 14:1131.

7. Chang, H. H. C., and Smith, M. C. (1960) On the drag of a spherical satellite moving in a partially ionized atmosphere, British Interplanetary Society J., 17:199.

8. Brundin, C. L. (1963) Effects of charged particles on the motion of an earth satellite, AIAA Journal, 1 (No. 11):2529.

9. Samir, U., Maier, E. J., and Troy, Jr., B. E. (1973) The angular distribution of ion flux around an ionospheric satellite, J. Atmos. and Terr. Physics, 35:513.

10. Kasha, M. A. (1969) The Ionosphere and its Interaction With Satellites, Chapter 3, New York, Gordon and Breach.

11. Parker, L. W. (1979) Plasma sheath effects and voltage distributions of large, high-power satellite solar arrays, Proceedings of the Spacecraft Charging Technology Conference, USAF Academy, Colorado Springs, Colo., 1978, p. 341, NASA Conference Publications 2071/AFGL-TR-79-0082.

33

12. Freeman, J. W., Cooke, D., and Reiff, P. (1979) Space environmental effects and the solar power satellite, *Proceedings of the Spacecraft Charging Technology Conference, USAF Academy, Colorado Springs, Colo., 1978*, p. 408, NASA Conference Publication 2071/AFGL-TR-79-0082.

13. Whipple, Jr., E. C. (1959) The ion trap results in the 'exploration of the upper atmosphere with the help of the third Soviet Sputnik,' *Proc. IRE*, 47:2023.

14. Sohn, M. (1959) Attitude stabilization by means of solar radiation pressure, *American Rocket Society J.*, **29**:371.

15. Renner, U. (1979) Attitude control by solar sailing - a promising experiment with OTS-2, *European Space Agency J.*, 3:35.

16. Cook, G. E. (1965) Satellite drag coefficients, *Planetary and Space Science*, 13:929.

17. Schamberg, R. (1959) Analytic representation of surface interaction for free molecule flow with application to drag of various bodies, in *Aerodynamics of the Upper Atmosphere*, edited by D. J. Masson, p. 12-1, Rand Corporation.

18. Epstein, P. S. (1924) Resistance experienced by spheres in their motion through gases, *Phys. Rev.*, **23**:710.

19. Jastrow, R., and Pearse, C. A. (1957) Atmospheric drag on the satellite, *J. Geophys. Res.*, **62**:413.

20. Fournier, G. (1970) Electric drag, *Planetary and Space Science*, 18:1035.

21. Knechtel, E. D., and Pitts, W. C. (1964) Experimental investigation of electric drag on satellites, *AIAA Journal*, 2 (No. 6):1148.

22. Fischell, R. E., and Mobley, F. F. (1964) A system for passive gravity - gradient stabilization of earth satellites, in *Progress in Astronautics and Aeronautics: Guidance and Control - II*, Vol. 13, p. 37, New York, Academic Press.

23. Thomson, W. T. (1962) Spin stabilization of attitude against gravity torque, *J. Astronautical Sciences*, 9:31.

24. Ginter, S., and Balas, M. (1978) Attitude stabilization of large flexible spacecraft, AIAA Paper No. 78-1285, in *Proceedings of AIAA Guidance and Control Conference, Palo Alto, CA, 1978*, AIAA, New York.

Appendix
ROTATION EFFECTS

Additional mechanisms come into play when a body in the space plasma has rotation about some internal point in addition to translational motion. These mechanisms have been studied principally for spherical bodies,[1] and are summarized here for completeness.

- Aerodynamic Torque: A spinning body will be decelerated by drag from the neutral particles impinging on its surface.[2] For a spherical body, the magnitude of torque resulting is negligible above about 600 km altitude when compared with the other mechanisms listed here.

- Surface Charge Torque: The geometry of any bound charge on a conducting body, induced by translational motion across a magnetic field, for example, maintains a fixed orientation in that field. If the body spins, the bound charge flows through it to maintain this fixed orientation. The energy required to overcome the electrical resistance to this current flow is taken

1. Wood, G. P., and Hohl, F. (1965) Electric potentials, forces and torques on bodies moving through rarefied plasmas, AIAA Paper 65-628, AIAA, New York.

2. Davis, A. H., and Harris, I. (1961) Interaction of a charged satellite with the ionosphere, in Rarefied Gas Dynamics, edited by L. Talbot, p. 691, Academic Press, New York.

from the kinetic energy of the body's rotation, and, therefore, a deceleration of the spin results. In the case of a sphere, however, this deceleration is many orders of magnitude less than all other torques due to rotation.

- Reflected Ion Torque: Ions that strike the body are accelerated as they approach it by the potential of the body with respect to the plasma. If they are neutralized and undergo diffuse reflection without significant thermal accommodation, they have a net increase in energy. The associated momentum loss to the body applies a force to it at the point of impact. If the ion flow is not symmetric about the center of mass, because of the potential distribution on the body, for example, then a decelerating torque is applied. For a sphere, this torque is some 3 orders of magnitude smaller than the eddy-current and magnetically induced torques.

- Coulomb Torque: Ions that are not reflected, but remain on the body after neutralization, also will cause a torque, if the moments of their impact are not symmetric about the body's center of mass. The magnitude of this torque for a spherical body is some 3 orders of magnitude less than the eddy current and induced torques which effectively determine the changes to the initial spin rate of an orbiting body.

- Eddy-Current Torque: The rotation of a body within a magnetic field generates internal eddy currents that interact with the magnetic field via Lorentz forces to give decelerating torques. These are the largest spin-reducing torques above about 600 km altitude. For the Echo II satellite, a 41-m-diam, segmented conducting sphere in a 1400-km circular orbit, the torque had a value on the order of 10^{-11} dyne cm.

- Magnetically Induced Torque: The currents flowing between the ambient plasma and a conducting body give rise to Lorentz forces as the body moves across a magnetic field. If the moments of these forces are not equally distributed about the center of mass, an accelerating torque will result, tending to spin up the body. In the case of Echo II, this torque was due to non-uniformities in the electrical resistance of the various segments from which the sphere was constructed, and was estimated to have a value on the order of 5×10^{10} dyne cm. Because the induced torque approximately equalized the decelerating eddy-current torques, the spin rate of Echo II remained almost constant for many months.

36